Human-Like Decision Making for Autonomous Driving: A Noncooperative Game Theoretic Approach

Peng Hang, Chen Lv, *Senior Member, IEEE*, Yang Xing, Chao Huang, and Zhongxu Hu

***Abstract*—Considering that human-driven vehicles and autonomous vehicles (AVs) will coexist on roads in the future for a long time, how to merge AVs into human drivers' traffic ecology and minimize the effect of AVs and their misfit with human drivers, are issues worthy of consideration. Moreover, different passengers have different needs for AVs, thus, how to provide personalized choices for different passengers is another issue for AVs. Therefore, a human-like decision making framework is designed for AVs in this paper. Different driving styles and social interaction characteristics are formulated for AVs regarding drive safety, ride comfort and travel efficiency, which are considered in the modelling process of decision making. Then, Nash equilibrium and Stackelberg game theory are applied to the noncooperative decision making. In addition, potential field method and model predictive control (MPC) are combined to deal with the motion prediction and planning for AVs, which provides predicted motion information for the decision-making module. Finally, two typical testing scenarios of lane change, i.e., merging and overtaking, are carried out to evaluate the feasibility and effectiveness of the proposed decision-making framework considering different human-like behaviors. Testing results indicate that this human-like decision making framework can make personalized decisions according to different driving styles.**

***Index Terms*—Decision making, human-like, autonomous vehicle, game theory, driver model, model predictive control.**

I. Introduction

DECISION making is a vital part of autonomous driving technology. According to the information provided by the environment perception module, proper driving behaviors are planned by the decision-making module and sent to the motion control module [1]. Therefore, decision making is usually regarded as the brain of AV and bridges environment perception and motion control. The driving performance of AVs is effectively affected by the decision-making module, including drive safety, ride comfort, travel efficiency, and energy consumption [2].

This work was supported in part by the SUG-NAP Grant (No. M4082268.050) of Nanyang Technological University, Singapore, and A*STAR Grant (No. 1922500046), Singapore.

P. Hang, C. Lv, C. Huang, J. Cai, Z Hu and Y. Xing are with the School of Mechanical and Aerospace Engineering, Nanyang Technological University, Singapore 639798. (e-mail: {peng.hang, lyuchen, xing.yang, chao.huang, zhongxu.hu}@ntu.edu.sg)

(Corresponding author: Chen Lv)

Many methods have been applied to the decision making of AVs in recent years. A probabilistic model is widely used to deal with the uncertainties of decision making [3], [4]. In [5], a Bayesian networks model is applied to decision making, that considers the uncertainties from environmental perception to decision making. However, it is difficult to deal with complex and dynamic decision missions. The Markov Decision Process (MDP) is another common probabilistic model for decision making. In [6], a robust decision-making approach is studied using partially observable MDP considering uncertain measurements, which can make AVs move safely and efficiently amid pedestrians. In [7], a stochastically verifiable decision-making framework is designed for AVs based on Probabilistic Timed Programs (PTPs) and Probabilistic Computational Tree Logic (PCTL). In addition, the Multiple Criteria Decision Making (MCDM) method and the Multiple Attribute Decision Making (MADM) method are effective to deal with complex urban environment and make reasonable decisions for AVs [8], [9].

With the development of machine learning algorithms, increasing numbers of learning-based decision-making methods have been studied. In [10], a kernel-based extreme learning machine (KELM) modeling method is proposed for speed decision making of AVs. In [11], a support vector machine (SVM) algorithm is applied to automatic decision making with Bayesian parameters optimization. In [12], a stochastic MDP is used to model the interaction between an AV and the environment, and reinforcement learning (RL) is then applied to decision making according to the reward function of MDP. A human-like decision-making system is built based on Deep Neural Networks (DNNs) in [13], which can adapt to real-life road conditions. Compared with DNNs and other learning algorithms, the RL method does not need large quantities of labeled data from drivers, as it is a self-learning framework that solves sequential decision-making problem by interacting with the environment [14]. A Q-learning (QL) decision-making method is proposed based on RL in [15]. However, the learning efficiency and generalization ability of QL need to be improved.

Moreover, rule-based decision-making methods have been studied by many researchers, including fuzzy logic and expert system. In [16], a prediction and cost function-based algorithm is proposed to deal with the decision-making problem of highway driving for AVs. A decision-making approach using

fuzzy logic is studied to address automatic overtaking in [17]. Rule-based decision-making methods are easy to conduct, while the robustness of algorithms is poor.

There are various driving scenarios for system design, algorithm evaluation, and performance verification of AVs. Considering that most traffic accidents on highways are caused by lane-change behaviors [18], lane change is regarded as a typical, common and potentially dangerous driving scenario to test AVs' performances in many studies [19]-[21]. Therefore, lane change is also studied as a target driving scenario in this paper.

Most of the aforementioned algorithms have been widely investigated to solve the lane-change decision-making problem for AVs. However, few of the algorithms consider the social interactions of vehicles in the decision-making process. Game theory is an effective approach to address this issue, especially under lane-change conditions [22]-[24]. A game theory-based lane-changing model is built in [25], which can make AV change lanes in a human-like manner. In [26], the interactions between the host vehicle and surrounding vehicles are captured in a game theoretic approach, which can make optimal lane-change decision to overtake, merge and avoid collisions. A lane-change model is conducted based on a game theoretic approach to address the cooperative control of connected vehicles through vehicle-to-vehicle communications [27].

To consider the social interactions between the AV and surrounding vehicles, in this study, a human-like decision making framework for AVs is built. Different driving styles are defined for AVs to simulate human-like driving behaviors in the decision-making process. Then, the decision making of AV is transformed into a noncooperative game. Nash equilibrium and Stackelberg game theory are utilized to address this problem. In addition, potential field method and model predictive control (MPC) are applied to motion prediction and planning, respectively, which are used to predict collision-avoidance path for the decision-making module. Finally, the human-like decision making framework for AVs is verified via different testing scenarios.

The rest of this paper is structured as follows. In Section II, the problem description and human-like system framework are presented. Then, the integrated model combining the driver model and the vehicle-road model is built in Section III. In Section IV, the decision-making module is established based on noncooperative game theory. Moreover, the motion prediction and planning module is designed using the potential field method and MPC in Section V. Test results and analysis of the proposed approach are discussed in Section VI. Finally, Section VII concludes the paper.

II. Problem Description and System Framework

Different human drivers have different driving styles due to their individual differences, i.e., different drivers may make different decisions under the same condition. For instance, in terms of the emergency collision avoidance condition, aggressive drivers may choose a quick steering behavior and timid drivers may choose a quick braking behavior. Additionally, different passengers prefer different driving styles. For instance, babies, pregnant women and order people prefer a comfortable and safe riding experience. Couriers care more about travel efficiency on the road. Therefore, the decision-making framework for AVs should not be fixed and unchanged. Instead, it should be human-like and adaptable for different passengers. However, driving styles are seldom considered during decision making process in existing studies.

For human drivers, driving styles are affected by both human factors and environmental factors, including physical limitations, habits, personality, age, road conditions, weather, etc. [28], [29]. In this paper, three driving styles are defined, i.e., aggressive, normal and conservative, which are used to design the human-like decision making framework for AVs. In general, aggressive drivers care more about the vehicle dynamic performance and travel efficiency. Namely, they would like to frequently rotate the steering wheel or step on the throttle and brake pedal. In contrast, conservative drivers give priority to driving safety and ride comfort. Therefore, they execute their actions very carefully. Normal drivers, wo are positioned between the above two driving styles, are likely to make a trade-off decision by considering travel efficiency, ride comfort and drive safety [30], [31].

With consideration of different driving styles, the decision-making framework for AVs is more human-friendly, which can provide personalized choices for different passengers in regard to drive safety, ride comfort and travel efficiency. Additionally, it can be expected that human-driven vehicles and AVs will coexist on the roads in the future for a long time. Safety is not the only requirement for AVs, how to merge into the traffic consisting of human drivers is another vital issue to be discussed. AVs should not behave too differently from surrounding human-driven vehicles. If AVs are human-like, surrounding human drivers can easily interact with AVs and predict their behaviors, particularly with regard to cooperative maneuvers. The aforementioned factors are the main reason that we want to design a human-like decision making framework for AVs.

Furthermore, the human-like decision making framework of lane change for AVs is illustrated in Fig. 1. In the modeling process of decision making, three different driving styles are reflected as drive safety, ride comfort and travel efficiency. Then, noncooperative game theory is used to make proper decisions for AVs. In the modelling process of human-like driving, driver model is adopted to describe different driving styles. Combined with potential model method, MPC is applied for motion prediction and planning, which aims to predict collision-avoidance path for the decision-making module.

The contributions of this paper are summarized as follows. 1. Different driving styles and social interaction characteristics are formulated for AVs and are taken into consideration in the modeling process of decision making. 2. A human-like decision making framework is designed for AVs based on the driver model and noncooperative game, and Nash equilibrium and Stackelberg game theory are used to solve the noncooperative decision-making problem. 3. The potential field method and MPC are applied to motion panning for AVs, which provide predicted motion information for the decision-making

framework.

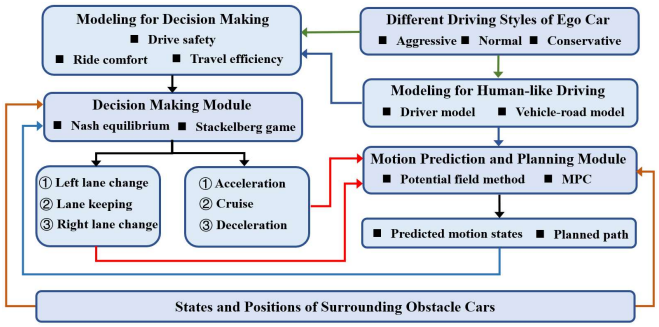

Fig. 1. Human-like decision making framework for AVs.

III. Modelling for Human-like Driving

In this section, different driving styles are described in the driver model. Then, the combination of the driver model and vehicle-road model yields an integrated model for human-like driving, which is applied to the motion prediction of AVs.

A. Driver Model

Fig. 2 shows a single-point preview driver model, that is widely used in vehicle control [32]. In this paper, the model is applied to the motion prediction of AVs. In Fig. 2, point E is the current position of the driver. φ is the yaw angle of the vehicle. M is the predicted point along the current moving direction of the vehicle in the future, which is predicted by the driver's brain according to the vehicle states and position. P is the preview point created by the driver's eyes, and consecutive preview points make up the planned path. The driver aims to minimize the distance between the predicted point and the preview point. Finally, the purpose is realized by controlling the steering angle of the front wheel. The aforementioned content describes the basic working principle of the driver model.

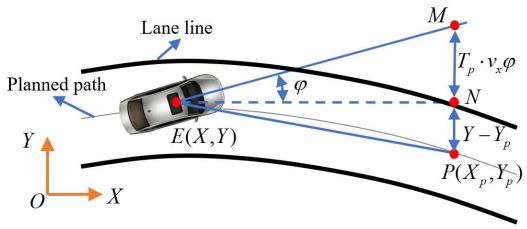

Fig. 2. Driver model.

Considering the driver's driving characteristics, the driver model is expressed as follows [33].

$$\ddot{\delta}_f = -\frac{1}{aT_d}\dot{\delta}_f - \frac{1}{aT_d^2}\delta_f + \frac{K_s G_s}{aT_d^2}[Y_p - (Y + T_p \cdot v_x\varphi)] \quad (1)$$

where δ_f is the steering angle of the front wheel, a is related to the damping rate of the model, T_d and T_p are the driver's physical delay time and predicted time, v_x is the longitudinal velocity of the vehicle, Y and Y_p are the lateral coordinate position of the vehicle and preview point, K_s is the transmission ratio of steering system, and G_s is the steering proportional gain. The driver's driving style or characteristic is reflected by T_d, T_p and G_s. For instance, conservative drivers require more time for mental signal processing and muscular activation than aggressive drivers. Therefore, conservative drivers have larger T_d. However, aggressive drivers have opposite reactions [34].

Referring to [35]-[37], the parameters that reflect different driving styles are selected in Table I.

TABLE I
Parameters of Different Driving Styles

Parameters	Aggressive	Normal	Conservative
T_d	0.14	0.18	0.24
T_p	1.02	0.94	0.83
G_s	0.84	0.75	0.62
a	0.24	0.23	0.22

To analyze the characteristic of the driver model with the different driving styles, the distance error between predicted point M and preview point P is denoted by ΔY, i.e., $\Delta Y = Y_p - (Y + T_p \cdot v_x\varphi)$. Then, the transfer function from ΔY to δ_f is derived as

$$\delta_f(s) = \frac{K_s G_s}{aT_d^2 s^2 + T_d s + 1}\Delta Y(s) \quad (2)$$

According to Eq. (2), Fig. 3 presents the step response results of the driver model under the three different driving styles. It can be seen that the aggressive style has the fastest response speed and the maximum stable gain. By comparison, the conservative style has the longest response time and the minimum stable gain. The response result of normal style is between the above two driving styles. From the aforementioned analysis, it can be concluded that aggressive drivers usually control the steering wheel with a large amplitude and high frequency. However, conservative drivers show the opposite behaviors.

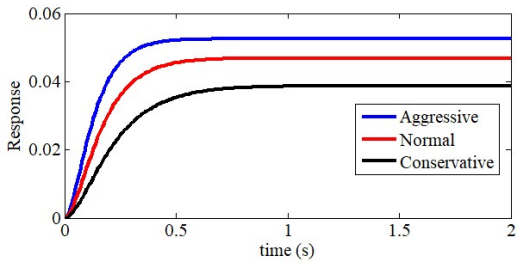

Fig. 3. Step response results of the driver model under the three driving styles.

B. Vehicle-Road Model

To reduce the complexity of the controller design, the four-wheel vehicle model is simplified as a two-wheel bicycle model [38], which is illustrated in Fig. 4.

Assuming that the steering angle of the front wheel δ_f has a small value, it yields $\sin\delta_f \approx 0$. According to Fig. 4, the simplified vehicle dynamic model is derived as follows [39].

$$\begin{cases} \dot{v}_x = v_y r + F_{xf}\cos\delta_f / m + F_{xr} / m \\ \dot{v}_y = -v_x r + F_{yf}\cos\delta_f / m + F_{yr} / m \\ \dot{r} = l_f F_{yf}\cos\delta_f - l_r F_{yr} \end{cases} \tag{3}$$

where v_y is the lateral velocity of the vehicle, and r is the yaw rate. $F_{xi}(i=f,r)$ and $F_{yi}(i=f,r)$ denote the longitudinal and lateral tire forces of the front and rear wheels. l_f and l_r are the front and rear wheel bases. m is the vehicle mass.

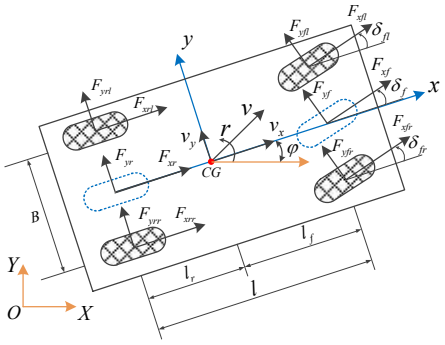

Fig. 4. Bicycle model.

If air resistance and tire rolling resistance are neglected, the longitudinal dynamics can be simplified as

$$a_x = F_{xf}\cos\delta_f / m + F_{xr} / m \tag{4}$$

With the assumption of a small tire slip angle, the relationship between the lateral tire force and the tire slip angle can be simplified as a linear relationship.

$$F_{yf} = -k_f \alpha_f, \quad F_{yr} = -k_r \alpha_r \tag{5}$$

where k_f and k_r are the cornering stiffness of the front and rear tires, respectively, and the slip angles of the front and rear tires α_f and α_r are defined by

$$\alpha_f = -\delta_f + (v_y + l_f r)/v_x, \quad \alpha_r = (v_y - l_r r)/v_x \tag{6}$$

In addition, the vehicle kinematic model in global coordinates is expressed as

$$\begin{cases} \dot{X} = v_x\cos\varphi - v_y\sin\varphi \\ \dot{Y} = v_x\sin\varphi + v_y\cos\varphi \\ \dot{\varphi} = r \end{cases} \tag{7}$$

C. Integrated Model for Human-like Driving

Combining the driver model and the vehicle-road model yields the integrated model for motion prediction. As Fig. 5 shows, the integrated model has two inputs, i.e., a_x and Y_p. a_x is the input of the vehicle-road model and Y_p is the input of the driver model, which await solution. The outputs of the integrated model are the vehicle states and position, which are used for decision making and motion planning.

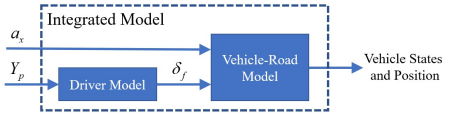

Fig. 5. Integrated model.

According to Eqs. (1), (3) and (7), the integrated model for motion prediction is expressed as.

$$\dot{x}(t) = f\left[x(t), u(t)\right] \tag{8}$$

$$f\left[x(t),u(t)\right] = \begin{bmatrix} v_y r + a_x \\ -v_x r + F_{yf}\cos\delta_f / m + F_{yr} / m \\ l_f F_{yf}\cos\delta_f - l_r F_{yr} \\ r \\ v_x\cos\varphi - v_y\sin\varphi \\ v_x\sin\varphi + v_y\cos\varphi \\ \dot{\delta}_f \\ -\dfrac{1}{aT_d^2}\delta_f - \dfrac{1}{aT_p}\dot{\delta}_f + \dfrac{R_g G_h}{aT_d^2}\left[Y_p - (Y - T_p\cdot v_x\varphi)\right] \end{bmatrix} \tag{9}$$

where the state vector $x = [v_x, v_y, r, \varphi, X, Y, \delta_f, \dot{\delta}_f]^T$, and the control vector $u = Y_p$.

IV. Decision Making Based on Noncooperative Game Theory

In this section, modelling for lane-change decision making is conducted considering different driving styles. Then, Nash equilibrium and Stackelberg game theory are applied to the noncooperative decision making. In the modelling process, the lane-change behaviors of obstacle vehicles are not included, thus only acceleration and deceleration behaviors are considered for obstacle vehicles.

A. Modeling for Lane-change Decision Making

Fig. 6 shows a common lane-change scenario on a three-lane highway. Ego car (EC) is an AV moving on the middle lane, and lead car 2 (LC2) moves in front of EC with a small velocity. EC has to decide to decelerate and follow LC2 or change lanes, then, change to the left lane or the right lane, which is a decision-making problem.

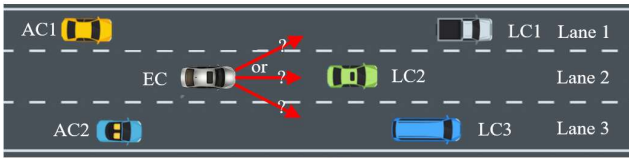

Fig. 6. Lane-change decision making.

Three performance indexes are taken into consideration in the modeling process of decision making, i.e., drive safety, ride comfort and travel efficiency. Therefore, the cost function of decision making for EC is the integration of these three components, which is expressed as

$$J^{EC}=w_{ds}^{EC}J_{ds}^{EC}+w_{rc}^{EC}J_{rc}^{EC}+w_{pe}^{EC}J_{pe}^{EC} \tag{10}$$

where J_{ds}^{EC}, J_{rc}^{EC} and J_{pe}^{EC} denote the costs of drive safety, ride comfort and travel efficiency, respectively. w_{ds}^{EC}, w_{rc}^{EC} and w_{pe}^{EC} are the weighting coefficients.

The drive safety cost of EC is made up of two parts, i.e., the longitudinal drive safety cost and the lateral drive safety cost, which are related to the lead car (LC) and adjacent car (AC), respectively. Furthermore, drive safety cost J_{ds}^{EV} is defined by

$$J_{ds}^{EC}=(\sigma^2-1)^2J_{ds-log}^{EC}+\sigma^2J_{ds-lat}^{EC} \tag{11}$$

where J_{ds-log}^{EC} and J_{ds-lat}^{EC} denote the longitudinal drive safety cost and the lateral drive safety cost, respectively. σ is the lane-change behavior of EC, $\sigma\in\{-1,0,1\}:=\{$*change left*, *no lane change*, *change right*$\}$.

The longitudinal drive safety cost J_{ds-log}^{EC} is a function of the longitudinal gap and relative velocity with respective to LC, which is defined by

$$J_{ds-log}^{EC}=\kappa_{v\text{-}log}^{EC}\lambda_{\upsilon}^{EC}/[(\Delta v_{x,\upsilon}^{EC})^2+\varepsilon]+\kappa_{s-log}^{EC}/[(\Delta s_{x,\upsilon}^{EC})^2+\varepsilon] \tag{12a}$$

$$\Delta v_{x,\upsilon}^{EC}=v_{x,\upsilon}^{LC}-v_{x,\upsilon}^{EC} \tag{12b}$$

$$\Delta s_{x,\upsilon}^{EC}=\sqrt{(X_{\upsilon}^{LC}-X_{\upsilon}^{EC})^2+(Y_{\upsilon}^{LC}-Y_{\upsilon}^{EC})^2}-l_v \tag{12c}$$

$$\lambda_{\upsilon}^{EC}=\begin{cases}1, & \Delta v_{x,\upsilon}^{EC}<0\\ 0, & \Delta v_{x,\upsilon}^{EC}\geq 0\end{cases} \tag{12d}$$

where $v_{x,\upsilon}^{LC}$ and $v_{x,\upsilon}^{EC}$ denote the longitudinal velocities of LC and EC, respectively. $(X_{\upsilon}^{LC},Y_{\upsilon}^{LC})$ and $(X_{\upsilon}^{EC},Y_{\upsilon}^{EC})$ are the positions of LC and EC, respectively. $\kappa_{v\text{-}log}^{EC}$ and κ_{s-log}^{EC} are the weighting coefficients. ε is a very small value to avoid zero denominator in the calculation. l_v is a safety coefficient considering the length of the car. υ denotes the lane number, $\upsilon\in\{1,2,3\}:=\{$*left lane*, *middle lane*, *right lane*$\}$.

The lateral drive safety cost J_{ds-lat}^{EC} is associated with the longitudinal gap and relative velocity with respective to AC, which is expressed as

$$J_{ds-lat}^{EC}=\kappa_{v\text{-}lat}^{EC}\lambda_{\upsilon+\sigma}^{EC}/[(\Delta v_{x,\upsilon+\sigma}^{EC})^2+\varepsilon]+\kappa_{s-lat}^{EC}/[(\Delta s_{x,\upsilon+\sigma}^{EC})^2+\varepsilon] \tag{13a}$$

$$\Delta v_{x,\upsilon+\sigma}^{EC}=v_{x,\delta}^{EC}-v_{x,\upsilon+\sigma}^{AC} \tag{13b}$$

$$\Delta s_{x,\upsilon+\sigma}^{EC}=\sqrt{(X_{\upsilon}^{EC}-X_{\upsilon+\sigma}^{AC})^2+(Y_{\upsilon}^{EC}-Y_{\upsilon+\sigma}^{AC})^2}-l_v \tag{13c}$$

$$\lambda_{\upsilon+\sigma}^{EC}=\begin{cases}1, & \Delta v_{x,\upsilon+\sigma}^{EC}<0\\ 0, & \Delta v_{x,\upsilon+\sigma}^{EC}\geq 0\end{cases} \tag{13d}$$

where $v_{x,\upsilon+\sigma}^{AC}$ is the longitudinal velocity of AC, $(X_{\delta+\alpha}^{AC},Y_{\delta+\alpha}^{AC})$ is the position of AC, $\kappa_{v\text{-}lat}^{EC}$ and κ_{s-lat}^{EC} are the weighting coefficients.

The ride comfort cost J_{rc}^{EC} is directly related to the longitudinal acceleration and lateral acceleration, which is defined by

$$J_{rc}^{EC}=\kappa_{a_x}^{EC}(a_{x,\upsilon}^{EC})^2+\sigma^2\kappa_{a_y}^{EC}(a_{y,\upsilon}^{EC})^2 \tag{14}$$

where $a_{x,\upsilon}^{EC}$ and $a_{y,\upsilon}^{EC}$ are the longitudinal acceleration and lateral acceleration of EC. $\kappa_{a_x}^{EC}$ and $\kappa_{a_y}^{EC}$ are the weighting coefficients.

The travel efficiency cost J_{pe}^{EC} is associated with the longitudinal velocity of EC, which is expressed as

$$J_{pe}^{EC}=(v_{x,\upsilon}^{EC}-\bar{v}_{x,\upsilon}^{EC})^2,\ \ \bar{v}_{x,\upsilon}^{EC}=\min(v_{x,\upsilon}^{\max},v_{x,\upsilon}^{LC}) \tag{15}$$

where $v_{x,\upsilon}^{\max}$ is the velocity limit on the lane υ.

Furthermore, the cost function for AC has a similar expression, which will not be introduced repeatedly. Two differences are noted. First, since it is assumed that AC does not change lanes and only assumes acceleration or deceleration behavior, the lateral drive safety cost of AC is equal to the lateral drive safety cost of EC. The ride comfort cost of AC only comes from longitudinal acceleration.

As mentioned in Section II, three different driving styles, i.e., aggressive, normal and conservative, are defined to describe the social behaviors of AV. In the modelling process of decision making, the differences between the different driving styles are reflected to different settings of weighting coefficients, i.e., w_{ds}^{EC}, w_{rc}^{EC} and w_{pe}^{EC}, which are related to drive safety, ride comfort and travel efficiency. Referring to [30], [31], the weighting coefficients of the three driving styles are shown in Table II.

TABLE II
WEIGHTING COEFFICIENTS OF THE DIFFERENT DRIVING STYLES

Weighting Coefficients	Aggressive	Normal	Conservative
w_{ds}^{EC}	10%	50%	70%
w_{rc}^{EC}	10%	30%	20%
w_{pe}^{EC}	80%	20%	10%

B. Noncooperative Decision Making Based on Nash Equilibrium

In common lane-change scenarios, the game problem occurs between EC and AC, which is a 2-player game problem. The noncooperative decision making based on Nash equilibrium for two players can be expressed as

$$(a_{x,\upsilon}^{EC*},\sigma^*)=\arg\min_{a_{x,\upsilon}^{EC},\sigma}J^{EC}(a_{x,\upsilon}^{EC},\sigma,a_{x,\upsilon+\sigma}^{AC}) \tag{16a}$$

$$a_{x,\upsilon+\sigma}^{AC*}=\arg\min_{a_{x,\upsilon+\sigma}^{AC}}J^{AC}(a_{x,\upsilon}^{EC},\sigma,a_{x,\upsilon+\sigma}^{AC}) \tag{16b}$$

$$\text{s.t.}\ \ \sigma\in\{-1,0,1\},\ \ a_{x,\upsilon}^{EC}\in[a_{x,\upsilon}^{\min},a_{x,\upsilon}^{\max}],\ \ a_{x,\upsilon+\sigma}^{AC}\in[a_{x,\upsilon+\sigma}^{\min},a_{x,\upsilon+\sigma}^{\max}],$$
$$v_{x,\upsilon}^{EC}\in[v_{x,\upsilon}^{\min},v_{x,\upsilon}^{\max}],\ \ v_{x,\upsilon+\sigma}^{AC}\in[v_{x,\upsilon+\sigma}^{\min},v_{x,\upsilon+\sigma}^{\max}].$$

where $a_{x,\upsilon}^{EC*}$ and $a_{x,\upsilon+\sigma}^{AC*}$ are the optimal longitudinal accelerations of EC and AC, σ^* is the optimal lane-change behavior of EC, $a_{x,i}^{\min}(i=\upsilon,\upsilon+\sigma)$ and $a_{x,\upsilon}^{\max}(i=\upsilon,\upsilon+\sigma)$ are

the minimum and maximum boundaries of longitudinal acceleration, $v_{x,i}^{\min}(i=\upsilon,\upsilon+\sigma)$ and $v_{x,\upsilon}^{\max}(i=\upsilon,\upsilon+\sigma)$ are the minimum and maximum constraints of longitudinal velocity.

If there are two ACs on the left and right lanes respectively as Fig. 6 shows, Eq. (16) should be rewritten as

$$(a_{x,\upsilon}^{EC*},\sigma^*)=\arg\min_{(a_{x,\upsilon}^{EC},\sigma)\in \mathrm{A}}[J_1,J_2] \tag{17a}$$

$$\mathrm{A}\triangleq\{(a_{x,\upsilon,1}^{EC},\sigma_1),(a_{x,\upsilon,2}^{EC},\sigma_2)\} \tag{17b}$$

$$J_1=\min_{a_{x,\upsilon,1}^{EC},\sigma_1} J^{EC}(a_{x,\upsilon,1}^{EC},\sigma_1,a_{x,\upsilon+\sigma_1}^{AC1}) \tag{17c}$$

$$J_2=\min_{a_{x,\upsilon,2}^{EC},\sigma_2} J^{EC}(a_{x,\upsilon,2}^{EC},\sigma_2,a_{x,\upsilon+\sigma_2}^{AC2}) \tag{17d}$$

$$a_{x,\upsilon+\sigma_1}^{AC1*}=\arg\min_{a_{x,\upsilon+\sigma_1}^{AC1}} J^{AC1}(a_{x,\upsilon,1}^{EC},\sigma_1,a_{x,\upsilon+\sigma_1}^{AC1}) \tag{17e}$$

$$a_{x,\upsilon+\sigma_2}^{AC2*}=\arg\min_{a_{x,\upsilon+\sigma_2}^{AC2}} J^{AC2}(a_{x,\upsilon,2}^{EC},\sigma_2,a_{x,\upsilon+\sigma_2}^{AC2}) \tag{17f}$$

$$\begin{aligned}\text{s.t. }\ & a_{x,\upsilon,1}^{EC},a_{x,\upsilon,2}^{EC}\in[a_{x,\upsilon}^{\min},a_{x,\upsilon}^{\max}],\ \ v_{x,\upsilon,1}^{EC},v_{x,\upsilon,2}^{EC}\in[v_{x,\upsilon}^{\min},v_{x,\upsilon}^{\max}],\\ & a_{x,\upsilon+\sigma_1}^{AC1}\in[a_{x,\upsilon+\sigma_1}^{\min},a_{x,\upsilon+\sigma_1}^{\max}],\ \ v_{x,\upsilon+\sigma_1}^{AC1}\in[v_{x,\upsilon+\sigma_1}^{\min},v_{x,\upsilon+\sigma_1}^{\max}],\\ & a_{x,\upsilon+\sigma_2}^{AC2}\in[a_{x,\upsilon+\sigma_2}^{\min},a_{x,\upsilon+\sigma_2}^{\max}],\ \ v_{x,\upsilon+\sigma_2}^{AC2}\in[v_{x,\upsilon+\sigma_2}^{\min},v_{x,\upsilon+\sigma_2}^{\max}],\\ & \sigma_1,\sigma_2\in\{-1,0,1\}.\end{aligned}$$

C. Noncooperative Decision Making Based on Stackelberg Equilibrium

In addition to Nash equilibrium, Stackelberg game is another noncooperative game approach [40], [41]. In Nash equilibrium, EC and AC are two equal and independent players. In the solving process, both EC and AC aim to minimize their own cost functions of decision making without considering the opponent's decision-making results. However, in Stackelberg equilibrium, EC is a leader player and AC is a follower player, the behavior of AC will affect the decision making of EC. Applying Stackelberg equilibrium into lane-change decision making, it yields

$$(a_{x,\upsilon}^{EC*},\sigma^*)=\arg\min_{a_{x,\upsilon}^{EC},\sigma}(\max_{a_{x,\upsilon+\sigma}^{AC}\in\gamma^2(a_{x,\upsilon+\sigma}^{AC},\sigma)} J^{EC}(a_{x,\upsilon}^{EC},\sigma,a_{x,\upsilon+\sigma}^{AC})) \tag{18a}$$

$$\begin{aligned}\gamma^2(a_{x,\upsilon}^{EC},\sigma)\triangleq\{&\zeta\in\Phi^2:J^{AC}(a_{x,\upsilon}^{EC},\sigma,\zeta)\le\\ &J^{AC}(a_{x,\upsilon}^{EC},\sigma,a_{x,\upsilon+\sigma}^{AC}),\forall a_{x,\upsilon+\sigma}^{AC}\in\Phi^2\}\end{aligned} \tag{18b}$$

$$\begin{aligned}\text{s.t. }\ & \sigma\in\{-1,0,1\},\ \ a_{x,\upsilon}^{EC}\in[a_{x,\upsilon}^{\min},a_{x,\upsilon}^{\max}],\ \ a_{x,\upsilon+\sigma}^{AC}\in[a_{x,\upsilon+\sigma}^{\min},a_{x,\upsilon+\sigma}^{\max}],\\ & v_{x,\upsilon}^{EC}\in[v_{x,\upsilon}^{\min},v_{x,\upsilon}^{\max}],\ \ v_{x,\upsilon+\sigma}^{AC}\in[v_{x,\upsilon+\sigma}^{\min},v_{x,\upsilon+\sigma}^{\max}].\end{aligned}$$

Similarly, if there are two ACs on the left and right lanes respectively as Fig. 6 shows, Eq. (18) should be rewritten as

$$\begin{aligned}(a_{x,\upsilon}^{EC*},\sigma^*)=\arg\min_{(a_{x,\upsilon}^{EC},\sigma)\in\mathrm{A}}[&J^{EC}(a_{x,\upsilon,1}^{EC},\sigma_1,a_{x,\upsilon+\sigma_1}^{AC1}),\\ &J^{EC}(a_{x,\upsilon,2}^{EC},\sigma_2,a_{x,\upsilon+\sigma_2}^{AC2})]\end{aligned} \tag{19a}$$

$$\mathrm{A}\triangleq\{(a_{x,\upsilon,1}^{EC},\sigma_1),(a_{x,\upsilon,2}^{EC},\sigma_2)\} \tag{19b}$$

$$(a_{x,\upsilon,1}^{EC},\sigma_1)=\arg\min_{a_{x,\upsilon,1}^{EC},\sigma_1}(\max_{a_{x,\upsilon+\sigma_1}^{AC1}\in\gamma_1^2(a_{x,\upsilon+\sigma_1}^{AC1},\sigma_1)} J^{EC}(a_{x,\upsilon,1}^{EC},\sigma_1,a_{x,\upsilon+\sigma_1}^{AC1})) \tag{19c}$$

$$\begin{aligned}\gamma_1^2(a_{x,\upsilon,1}^{EC},\sigma_1)\triangleq\{&\zeta_1\in\Phi_1^2:J^{AC1}(a_{x,\upsilon,1}^{EC},\sigma_1,\zeta_1)\le\\ &J^{AC1}(a_{x,\upsilon,1}^{EC},\sigma_1,a_{x,\upsilon+\sigma_1}^{AC1}),\forall a_{x,\upsilon+\sigma_1}^{AC1}\in\Phi_1^2\}\end{aligned} \tag{19d}$$

$$(a_{x,\upsilon,2}^{EC},\sigma_2)=\arg\min_{a_{x,\upsilon,2}^{EC},\sigma_2}(\max_{a_{x,\upsilon+\sigma_2}^{AC2}\in\gamma_2^2(a_{x,\upsilon+\sigma_2}^{AC2},\sigma_2)} J^{EC}(a_{x,\upsilon,2}^{EC},\sigma_2,a_{x,\upsilon+\sigma_2}^{AC2})) \tag{19e}$$

$$\begin{aligned}\gamma_2^2(a_{x,\upsilon,2}^{EC},\sigma_2)\triangleq\{&\zeta_2\in\Phi_2^2:J^{AC2}(a_{x,\upsilon,2}^{EC},\sigma_2,\zeta_2)\le\\ &J^{AC2}(a_{x,\upsilon,2}^{EC},\sigma_2,a_{x,\upsilon+\sigma_2}^{AC2}),\forall a_{x,\upsilon+\sigma_2}^{AC2}\in\Phi_2^2\}\end{aligned} \tag{19f}$$

$$\begin{aligned}\text{s.t. }\ & a_{x,\upsilon,1}^{EC},a_{x,\upsilon,2}^{EC}\in[a_{x,\upsilon}^{\min},a_{x,\upsilon}^{\max}],\ \ v_{x,\upsilon,1}^{EC},v_{x,\upsilon,2}^{EC}\in[v_{x,\upsilon}^{\min},v_{x,\upsilon}^{\max}],\\ & a_{x,\upsilon+\sigma_1}^{AC1}\in[a_{x,\upsilon+\sigma_1}^{\min},a_{x,\upsilon+\sigma_1}^{\max}],\ \ v_{x,\upsilon+\sigma_1}^{AC1}\in[v_{x,\upsilon+\sigma_1}^{\min},v_{x,\upsilon+\sigma_1}^{\max}],\\ & a_{x,\upsilon+\sigma_2}^{AC2}\in[a_{x,\upsilon+\sigma_2}^{\min},a_{x,\upsilon+\sigma_2}^{\max}],\ \ v_{x,\upsilon+\sigma_2}^{AC2}\in[v_{x,\upsilon+\sigma_2}^{\min},v_{x,\upsilon+\sigma_2}^{\max}],\\ & \sigma_1,\sigma_2\in\{-1,0,1\}.\end{aligned}$$

V. Motion Prediction and Planning Based on the Potential Field Model Method and MPC

The potential field method is able to deal with the dynamic modeling of obstacles and roads, which is an effective method for motion planning. In this section, the potential field method is combined with MPC to predict the motion states and collision-avoidance path for the decision-making framework.

A. Potential Field Method for Collision Avoidance

The integrated potential field function of obstacle cars (OCs) and roads is expressed as

$$\Gamma(X,Y)=\sum_{i=1}^{n_1}\Gamma_i^{oc}(X,Y)+\sum_{j=1}^{n_2}\Gamma_j^{r}(X,Y) \tag{20}$$

where n_1 and n_2 are the numbers of OCs and lane lines, respectively. OCs include LVs and ACs.

$\Gamma^{oc}(X,Y)$ is the potential field function of the OC at the position (X,Y) in the global coordinates, which is defined as follows [42].

$$\Gamma^{oc}(X,Y)=a^{oc}\cdot\exp(\vartheta) \tag{21}$$

where

$$\vartheta=-\left\{\frac{\hat{X}^2}{2\rho_X^2}+\frac{\hat{Y}^2}{2\rho_Y^2}\right\}^b+cv_x^{oc}\gamma,\ \ \gamma=k^{oc}\frac{\hat{X}^2}{2\rho_X^2}\Big/\sqrt{\frac{\hat{X}^2}{2\rho_X^2}+\frac{\hat{Y}^2}{2\rho_Y^2}},$$

$$k^{oc}=\begin{cases}-1, & \hat{X}<0\\ 1, & \hat{X}\ge 0\end{cases},\ \ \begin{bmatrix}\hat{X}\\ \hat{Y}\end{bmatrix}=\begin{bmatrix}\cos\varphi^{oc} & \sin\varphi^{oc}\\ -\sin\varphi^{oc} & \cos\varphi^{oc}\end{bmatrix}\begin{bmatrix}X-X^{oc}\\ Y-Y^{oc}\end{bmatrix}.$$

(X^{oc},Y^{oc}) is the CoG (center of gravity) position of OC. a^{oc} is the maximum potential field value of OC. ρ_X and ρ_Y are the convergence coefficients. φ^{oc} and v_x^{oc} are the heading angle and longitudinal velocity of OC. b is the shape coefficient.

$\Gamma^{r}(X,Y)$ is the potential field function of the road, which is defined by

$$\Gamma^{r}(X,Y)=a^{r}\cdot\exp(-d+d^{\dagger}+0.5W) \tag{22}$$

where a^r is the maximum potential field value of the road, d is the minimum distance from the position (X,Y) to the lane line, $d^{\dagger}$ is the safety threshold value and W is the width of OC.

B. Motion Prediction Based on MPC

To conduct motion prediction using MPC, the integrated model, i.e., Eq. (9) is transformed into a time-varying linear system.

$$\dot{x}(t) = A_t x(t) + B_t u(t) \tag{23}$$

where the time-varying coefficient matrices are given by

$$A_t = \left.\frac{\partial f}{\partial x}\right|_{x_t, u_t}, \quad B_t = \left.\frac{\partial f}{\partial u}\right|_{x_t, u_t} \tag{24}$$

Furthermore, Eq. (23) can be discretized as

$$\begin{cases} x(k+1) = A_k x(k) + B_k u(k) \\ u(k) = u(k-1) + \Delta u(k) \end{cases} \tag{25}$$

where $A_k = e^{A_t \Delta T}$, $B_k = \int_0^{\Delta T} e^{A_t \tau} B_t d\tau$, ΔT is the sampling time, $x(k)=[v_{x,\upsilon}^{EC}(k), v_{y,\upsilon}^{EC}(k), r_{\upsilon}^{EC}(k), \varphi_{\upsilon}^{EC}(k), X_{\upsilon}^{EC}(k), Y_{\upsilon}^{EC}(k), \delta_{f,\upsilon}^{EC}(k), \dot{\delta}_{f,\upsilon}^{EC}(k)]^T$, $u(k)=Y_{p,\upsilon}^{EC}$, $\Delta u(k)=\Delta Y_{p,\upsilon}^{EC}$.

In addition, the output vector is defined by $y(k)=[y_1(k), y_2(k), y_3(k)]^T$, where $y_1(k)$ is the potential field value associated with the predicted position of EC, i.e., $y_1(k) = \Gamma(X_{\upsilon}^{EC}(k), Y_{\upsilon}^{EC}(k))$, and $y_2(k)$ and $y_3(k)$ are the lateral distance error and yaw angle error between the predicted position of EC and the center line of the lane υ, respectively.

Moreover, the predictive horizon N_p and the control horizon N_c are defined, $N_p \geq N_c$. At the time step *k*, the sate sequence, output sequence and control sequence are given by

$$x(k+1|k), x(k+2|k), \cdots, x(k+N_p|k) \tag{26a}$$

$$y(k+1|k), y(k+2|k), \cdots, y(k+N_p|k) \tag{26b}$$

$$\Delta u(k|k), \Delta u(k+1|k), \cdots, \Delta u(k+N_c-1|k) \tag{26c}$$

The cost function for motion prediction of EC is defined by

$$\Theta(k) = \sum_{i=1}^{N_p} \| y(k+i|k) \|_Q^2 + \sum_{j=0}^{N_c-1} \| \Delta u(k+j|k) \|_R^2 \tag{27}$$

where Q is the output weighting matrix, and R is the control variation weighting matrix.

Finally, the motion prediction and planning problem of EC can be expressed as

$$\Delta \mathbf{u}(k) = \arg\min_{\Delta \mathbf{u}(k)} \Theta(k) \tag{28}$$

s.t.

$$x(k+i|k) = A_k x(k+i-1|k) + B_k u(k+i-1|k),$$

$$y(k+i-1|k)=[y_1(k+i-1|k), y_2(k+i-1|k), y_3(k+i-1|k)]^T, \quad (i=1,2,\cdots,N_p),$$

$$u(k+i|k) = u(k+i-1|k) + \Delta u(k+i|k),$$

$$u_{\min} \leq u(k+i|k) \leq u_{\max},$$

$$\Delta u_{\min} \leq \Delta u(k+i|k) \leq \Delta u_{\max}, \quad (i=0,2,\cdots,N_c-1).$$

where $u_{\min}$ and $u_{\max}$ are the minimum and maximum constraints of u, $\Delta u_{\min}$ and $\Delta u_{\max}$ are the minimum and maximum constraints of Δu. After solving the multi-constraint optimization problem, the sequence of optimal input increments is obtained.

$$\Delta \mathbf{u}^*(k) = [\Delta u^*(k|k), \Delta u^*(k+1|k), \cdots, \Delta u^*(k+N_c-1|k)] \tag{29}$$

Then, the control output at the time step *k* can be calculated.

$$u(k|k) = u(k-1|k-1) + \Delta u^*(k|k) \tag{30}$$

Furthermore, the state vector can be updated according to Eq. (23). In another words, the motion prediction of EC is realized. At the next time step $k+1$, a new optimization is solved over a shifted prediction horizon with the updated state $x(k+1|k+1)$. The aforementioned optimization problem with multi-constraints can be solved by the *fmincon* function in MATLAB simulation environment.

VI. Testing Results and Performance Evaluation

In this section, two testing scenarios are designed to evaluate the feasibility and effectiveness of the proposed human-like decision making framework for AVs. All the driving scenarios are built and tested on the MATLAB-Simulink platform.

A. Scenario A

As Fig. 7 shows, Scenario A is a merging maneuver on a highway. In this scenario, EC has to change lanes due to the impending ending of the current lane. However, there exits an AC on the left lane. The decision making of EC must consider the reaction behavior of AC. In addition, the different driving styles of EC have significant effects on decision making. At the initial moment, the longitudinal velocities of EC and AC are 20 m/s and 15 m/s, and the initial gap between EC and AC is 2 m (EC is in front of AC). The testing results are demonstrated in Figs. 8-10 and Table III.

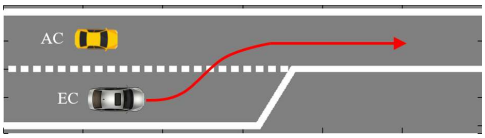

Fig. 7. Testing Scenario A.

It can be seen that the different driving styles and different decision-making strategies would lead to different testing results of decision making and motion planning. If EC is aggressive, EC would choose a sudden large acceleration to increase the gap immediately. Then, a lane-change behavior would be conducted. If the driving style of EC is normal, EC would not speed up with a large acceleration. It would like to accelerate progressively and increase the gap. When the gap is large enough, a lane-change maneuver would be carried out. In contrast, it would cause the opposite decision-making result if EC is conservative. It can be seen from Fig. 10 that EC would choose deceleration to guarantee drive safety. When EC moves close to the end of the current lane, the velocity of EC is much smaller than that of AC.

It is safe enough for EC to perform a merging maneuver. From Table III, it can also be found that aggressive mode has the smallest decision-making time and largest velocity for lane change, which indicates that aggressive mode cares more about travel efficiency. However, the conservative mode would spend more time decelerating to improve drive safety.

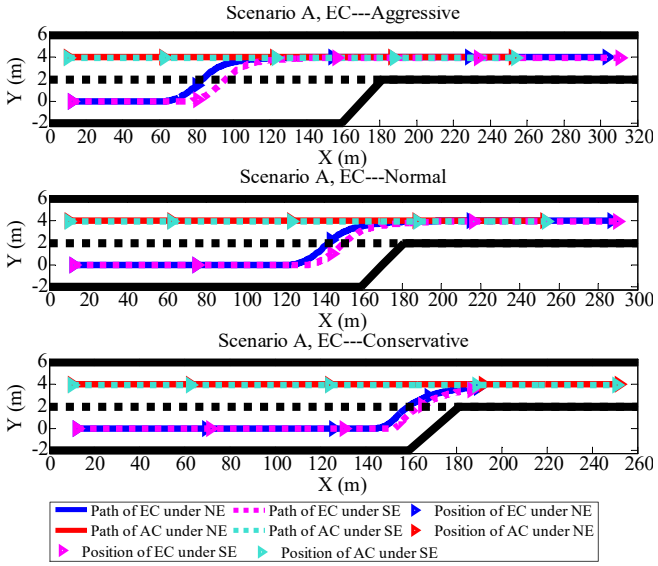

Fig. 8. Testing results of decision making considering different driving styles in Scenario A.

TABLE III
TEST RESULTS OF DECISION MAKING IN SCENARIO A

Testing Parameters	Aggressive		Normal		Conservative	
	NE	SE	NE	SE	NE	SE
t_c / s	2.24	2.72	5.04	5.36	7.00	7.18
Δs_{t_c} / m	13.77	16.46	18.06	18.86	-1.37	-1.99
v_{x,t_c}^{EC} / (m/s)	24.15	24.83	23.25	23.40	17.03	11.07
v_{x,t_c}^{AC} / (m/s)	18.66	19.17	20.76	20.91	21.49	21.52

where t_c is the time of lane-change decision making, Δs_{t_c} is the gap between EC and AC at the time t_c. v_{x,t_c}^{EC} and v_{x,t_c}^{AC} are the velocities of EC and AC at the time t_c. NE denotes Nash Equilibrium and SE denotes Stackelberg Equilibrium.

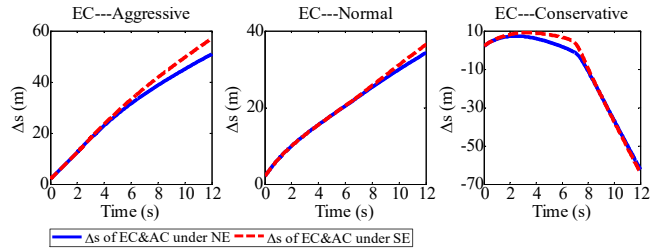

Fig. 9. Testing results of Δs in Scenario A.

Nash Equilibrium (NE) and Stackelberg Equilibrium (SE) are two different noncooperative game strategies for lane-change decision making. In NE, EC and AC are two equal and independent players. Both EC and AC aim to minimize their own cost functions of decision making. However, EC is the lead player in SE and AC is a follower player, the behavior of AC will affect the decision making of EC. Compared with NE, SE has a larger safe gap when performing a merging maneuver, which indicates that SE shows more consideration for safety in the decision-making process since the behavior of AC is fed back to the decision making of EC. In summary, SE decision making is more human-like, since human driver would adjust his decision making according to the behaviors of the surrounding vehicles.

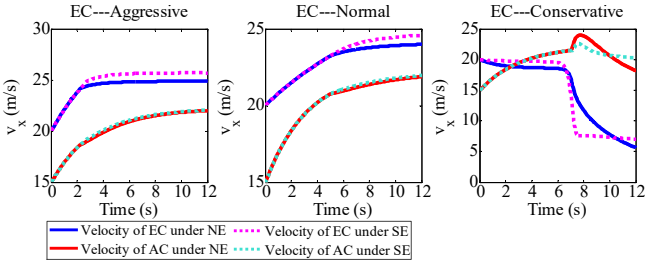

Fig. 10. Testing results of velocities in Scenario A.

B. *Scenario B*

Scenario B is an overtaking maneuver on a curved highway with three lanes. As Fig. 11 shows, both LC and EC move on the middle lane. Since LC moves with a slow velocity, EC has to a make decision, slowing down to maintain a safe distance and following LC on the current lane or changing lanes to overtake. If EC chooses to change lanes, which side should be selected, the left side or the right side? AC1 and AC2 are moving on the left and right lanes. The behaviors of both AC1 and AC2 must be taken into consideration in the decision-making process of EC. At the initial moment, the longitudinal velocities of LC, EC, AC1 and AC2 are set as 15 m/s, 20 m/s, 15 m/s and 13 m/s. The initial position coordinates of LC, EC, AC1 and AC2 are (62, 0.95), (12, 0.04), (10, 4.03), and (15, -3.94). Figs. 12-14 and Table IV show the detailed testing results under the different driving styles of EC and different decision-making strategies.

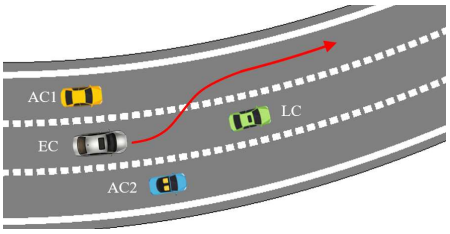

Fig. 11. Testing Scenario B.

TABLE IV
TEST RESULTS OF DECISION MAKING IN SCENARIO B

Testing Parameters	Aggressive		Normal		Conservative	
	NE	SE	NE	SE	NE	SE
t_c / s	2.98	3.44	3.90	4.20	-	-
$\Delta s_{t_c}^1$ / m	28.66	33.32	25.53	26.20	-	-
$\Delta s_{t_c}^2$ / m	26.22	31.21	22.55	24.06	-	-
v_{x,t_c}^{EC} / (m/s)	27.03	27.22	23.43	23.44	-	-
v_{x,t_c}^{AC1} / (m/s)	16.96	17.22	20.11	20.31	-	-
v_{x,t_c}^{AC2} / (m/s)	16.23	16.52	19.82	20.04	-	-

where t_c is the time of lane-change decision making, $\Delta s_{t_c}^i (i=1,2)$ denotes the gap between EC and ACi $(i=1,2)$ at the time t_c. v_{x,t_c}^{EC} and $v_{x,t_c}^{ACi} (i=1,2)$ denote the velocities of EC and ACi $(i=1,2)$ at the time t_c.

In this scenario, we also study the effect of the different driving styles on decision making for EC. Similar to Scenario A, if EC's driving style is set as aggressive, to improve travel efficiency, EC would speed up with a large acceleration and spend the shortest time finishing the overtaking process. If EC's driving style is set as normal, it would take more time to accelerate to create a larger safe gap for overtaking. However, if EC's driving style is set as conservative, EC prefers to decelerate to keep a larger safe distance between the other obstacle cars. Therefore, we can see from Figs 12 and 13 that EC does not change lanes at 10s in spite of the large gap of more than 20m. To explain this situation according to the decision-making model, the cost function of the lane-change for EC with a conservative driving style is larger than that of lane-keeping at this moment. In other words, EC with the conservative driving style cares more about drive safety rather than travel efficiency. In addition, we can see from Fig. 12 that EC would choose the left-side lane change due to the smaller cost generated for the left lane. Similar to Scenario A, it can be seen from Table IV that SE has larger t_c and $\Delta s_{t_c}^i$ value than NE, which indicates that SE shows more consideration of safety for EC in the process of decision making.

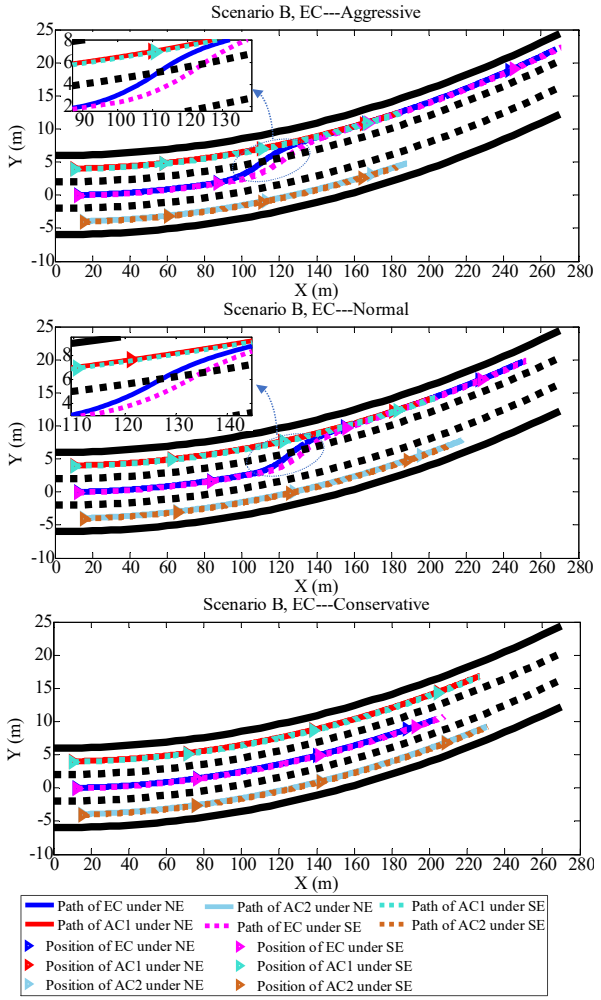

Fig. 12. Testing results of decision making considering different driving styles in Scenario B.

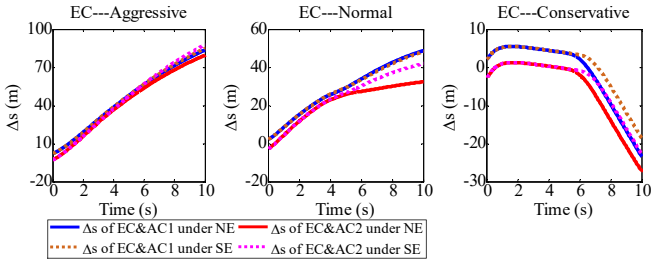

Fig. 13. Testing results of Δs in Scenario B.

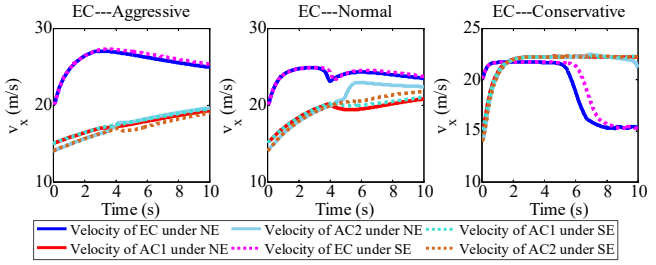

Fig. 14. Testing results of velocities in Scenario B.

VII. Conclusions

This paper presents a human-like decision making framework for AVs. Different driving styles associated with drive safety, ride comfort and travel efficiency are defined for AVs. Based on the decision-making model considering the different driving styles and social interaction characteristics, Nash equilibrium and Stackelberg game theory are utilized to address the noncooperative decision making problem. In addition, the potential field method and MPC are used to plan the collision-avoidance path and provide predicted motion states for the human-like decision making module. Finally, two testing scenarios are established to evaluate the performance of the decision-making framework. The testing results indicates that the developed framework is able to make reasonable decisions under different driving styles, which is human-like and can provide personalized choices for different passengers.

References

[1] Y. Huang, H. Wang, A. Khajepour, H. Ding, K. Yuan, and Y. Qin, "A novel local motion planning framework for autonomous vehicles based on resistance network and model predictive control," *IEEE Trans. Veh. Technol.*, vol. 69, no.1, pp. 55–66, Jan. 2020.

[2] F. Fabiani, and S. Grammatico, "Multi-vehicle automated driving as a generalized mixed-integer potential game," *IEEE Trans. Intell. Transp. Syst.*, vol. 21, no. 3, pp. 1064–1073, Mar. 2020.

[3] R. Schubert, "Evaluating the utility of driving: Toward automated decision making under uncertainty," *IEEE Trans. Intell. Transp. Syst.*, vol. 13, no. 1, pp. 354–364, Mar. 2012.

[4] S. Noh, "Decision-making framework for autonomous driving at road intersections: Safeguarding against collision, overly conservative behavior, and violation vehicles," *IEEE Trans Ind Electron*, vol. 66, no. 4, pp. 3275–3286, Apr. 2018.

[5] C Yu, X Wang, X Xu, M. Zhang, H. Ge, J. Ren, L. Sun, B. Chen, and G. Tan, "Distributed multiagent coordinated learning for autonomous driving in highways based on dynamic coordination graphs," *IEEE Trans. Intell. Transp. Syst.*, vol. 21, no. 2, pp. 735–748, Feb. 2020.

[6] H. Bai, S. Cai, N. Ye, D. Hsu, and W. S. Lee, "Intention-aware online POMDP planning for autonomous driving in a crowd," in *Proc IEEE Int Conf Rob Autom.*, Seattle, WA, United States, May. 2015, pp. 454–460.

[7] T. Rosenstatter, and C. Englund, "Modelling the level of trust in a cooperative automated vehicle control system," *IEEE Trans. Intell. Transp. Syst.*, vol. 19, no. 4, pp. 1237–1247, Apr. 2018.

[8] A. Furda and L. Vlacic, "Enabling safe autonomous driving in real-world city traffic using multiple criteria decision making," *IEEE Intell. Transp. Syst. Mag.*, vol. 3, no. 1, pp. 4–17, Apr. 2011.

[9] J. Chen, P. Zhao, H. Liang, and T. Mei, "A multiple attribute-based decision making model for autonomous vehicle in urban environment," in *Proc IEEE Intell Veh Symp*, Dearborn, MI, United States, June. 2014, pp. 480–485.

[10] X. Wu, X. Xu, X. Li, K. Li, and B. Jiang, "A kernel-based extreme learning modeling method for speed decision making of autonomous land vehicles," in *2017 6th Data Driven Control and Learning Systems (DDCLS)*, Chongqing, China, May. 2017, pp. 769–775.

[11] Y. Liu, X. Wang, L. Li, S. Cheng, and Z. Chen, "A novel lane change decision-making model of autonomous vehicle based on support vector machine," *IEEE Access*, vol. 7, pp. 26543–26550, 2019.

[12] C. You, J. Lu, D. Filev, and P. Tsiotras, "Highway traffic modeling and decision making for autonomous vehicle using reinforcement learning," in *Proc. IEEE Intell. Veh. Symp.*, Changshu, China, June. 2018, pp. 1227–1232.

[13] L. Li, K. Ota, and M. Dong, "Humanlike driving: Empirical decision-making system for autonomous vehicles," *IEEE Trans. Veh. Technol.*, vol. 67, no. 8, pp. 6814–6823, Aug. 2018.

[14] X. Xu, L. Zuo, X. Li, L. Qian, J. Ren, and Z. Sun, "A reinforcement learning approach to autonomous decision making of intelligent vehicles on highways," *IEEE Trans. Syst. Man Cybern. Syst*., to be published, Doi: 10.1109/TSMC.2018.2870983

[15] D. C. K. Ngai and N. H. C. Yung, "A multiple-goal reinforcement learning method for complex vehicle overtaking maneuvers," *IEEE Trans. Intell. Transp. Syst.*, vol. 12, no. 2, pp. 509–522, Jun. 2011.

[16] J. Wei and J. M. Dolan, "A robust autonomous freeway driving algorithm," in *Proc. IEEE Intell. Veh. Symp.*, Xi'an, China, June. 2009, pp. 1015–1020.

[17] J. Pérez, V. Milanés, E. Onieva, J. Godoy, and J. Alonso, "Longitudinal fuzzy control for autonomous overtaking," in Proc. IEEE Int. Conf. Mechatronics, Istanbul, Turkey, Apr. 2011, pp. 188–193.

[18] B. Sen, J. D. Smith, and G. W. Najm, ''Analysis of lane change crashes,'' *Nat. Highway Traffic Saf. Admin*., Washington, DC, USA, Tech. Rep. DOT HS 809 571, 2003.

[19] C. Hatipoglu, U. Ozguner, and K. A. Redmill, "Automated lane change controller design," *IEEE Trans. Intell. Transp. Syst.*, vol. 4, no. 1, pp. 13–22, Mar. 2003.

[20] J. E. Naranjo, C. Gonzalez, R. Garcia, and T. de Pedro, "Lane-change fuzzy control in autonomous vehicles for the overtaking maneuver," *IEEE Trans. Intell. Transp. Syst.*, vol. 9, no. 3, pp. 438–450, Sept. 2008.

[21] T. Shamir, "How should an autonomous vehicle overtake a slower moving vehicle: Design and analysis of an optimal trajectory," *IEEE Trans Autom Control*, vol. 49, no. 4, pp. 607–610, Apr. 2004.

[22] J. H. Yoo, and R. Langari, "Stackelberg game based model of highway driving," in *ASME Annu. Dyn. Syst. Control Conf. Jt. JSME Motion Vib. Conf.*, FL, United States, Oct. 2012, pp. 499–508.

[23] C. L. Darby, W. W. Hager, and A. V. Rao, "An hp-adaptive pseudospectral method for solving optimal control problems," *Optim Control Appl Methods*, vol. 32, no. 4, pp. 476–502, July. 2012.

[24] J. H. Yoo and R. Langari, "A Stackelberg game theoretic driver model for merging," in *ASME Dyn. Syst. Control Conf.*, Palo Alto, CA, United States, Oct. 2013.

[25] H. Yu, H. E. Tseng, and R. Langari, "A human-like game theory-based controller for automatic lane changing," *Transp. Res. Part C Emerg. Technol.*, vol. 88, pp. 140–158, Mar. 2018.

[26] M. Wang, S. P. Hoogendoorn, W. Daamen, B. van Arem, and R. Happee, "Game theoretic approach for predictive lane-changing and car-following control," *Transp. Res. Part C Emerg. Technol.*, vol. 58, pp. 73–92, Sept. 2015.

[27] A. Talebpour, H. S. Mahmassani, and S. H. Hamdar, "Modeling lane-changing behavior in a connected environment: A game theory approach," *Transp. Res. Part C Emerg. Technol.*, vol. 59, pp. 216–232, Oct. 2015.

[28] K. Driggs-Campbell, V. Govindarajan, and R. Bajcsy, "Integrating intuitive driver models in autonomous planning for interactive maneuvers," *IEEE Trans. Intell. Transp. Syst.*, vol. 18, no. 12, pp. 3461–3472, Dec. 2017

[29] J. Wang, G. Zhang, R. Wang, S. C. Schnelle, and J. Wang, "A gain-scheduling driver assistance trajectory-following algorithm considering different driver steering characteristics," *IEEE Trans. Intell. Transp. Syst.*, vol. 18, no. 5, pp. 1097–1108, May. 2017.

[30] C. Lv, X. Hu, A. Sangiovanni-Vincentelli, Y. Li, C. M. Martinez, and D. Cao, "Driving-style-based codesign optimization of an automated electric vehicle: a cyber-physical system approach," *IEEE Trans. Ind. Electron.*, vol. 66, no. 4, pp. 2965–2975, Apr. 2018.

[31] C. M. Martinez, M. Heucke, F. Y. Wang, B. Gao, and D. Cao, "Driving style recognition for intelligent vehicle control and advanced driver assistance: A survey," *IEEE Trans. Intell. Transp. Syst.*, vol. 19, no. 3, pp. 666–676, Aug. 2017.

[32] J. Wang, M. Dai, G. Yin, N. Chen, "Output-feedback robust control for vehicle path tracking considering different human drivers' characteristics," *Mechatronics*, vol. 50, pp. 402–412, Apr. 2018.

[33] K. Zhang, J. Wang, N. Chen, and G. Yin, "A non-cooperative vehicle-to-vehicle trajectory-planning algorithm with consideration of driver's characteristics," *Proc. Inst. Mech. Eng. Part D J. Automob. Eng.*, vol. 233, no. 10, pp. 2405–2420, July. 2018.

[34] Y. W. Chai, Y. Abe, Y. Kano, and M. Aeb, "A study on adaptation of SBW parameters to individual driver's steer characteristics for improved driver-vehicle system performance," *Veh Syst Dyn*, vol. 44, no. sup1, pp. 874–882, 2006.

[35] J. Wang, J. Wang, R. Wang, and C. Hu, "A framework of vehicle trajectory replanning in lane exchanging with considerations of driver characteristics," *IEEE Trans. Veh. Technol.*, vol. 66, no. 5, pp. 3583–3596, May. 2017.

[36] B. Zhou, Y. Wang, G. Yu, and X. Wu, "A lane-change trajectory model from drivers' vision view," *Transp. Res. Part C Emerg. Technol.*, vol. 85, pp. 609–627, Dec. 2017.

[37] B. Shi, L. Xu, J. Hu, Y. Tang, H. Jiang, W. Meng, and H. Liu, "Evaluating driving styles by normalizing driving behavior based on personalized driver modeling," *IEEE Trans. Syst. Man Cybern. Syst*., vol. 45, no. 12, pp. 1502–1508, Apr. 2015.

[38] P. Hang, and X. Chen, "Integrated chassis control algorithm design for path tracking based on four-wheel steering and direct yaw-moment control," *Proc Inst Mech Eng Part I J Syst Control Eng*, vol. 233, no. 6, pp. 625–641, Jul. 2019.

[39] P. Hang, X. Chen, and F. Luo, "LPV/H∞ controller design for path tracking of autonomous ground vehicles through four-wheel steering and direct yaw-moment control," *Int. J. Automot. Technol*., vol.20, no. 4, pp. 679–691, Aug. 2019.

[40] X. Na, and D. J. Cole, "Game-theoretic modeling of the steering interaction between a human driver and a vehicle collision avoidance controller," *IEEE Trans. Hum.-Mach. Syst*., vol. 45, no. 1, pp. 25–38, Feb. 2015.

[41] X. Na, and D. J. Cole, "Application of open-loop stackelberg equilibrium to modeling a driver's interaction with vehicle active steering control in obstacle avoidance," *IEEE Trans. Hum.-Mach. Syst.*, 2017, vol. 47, no. 5, pp. 673–685, May. 2017.

[42] Q. Tu, H. Chen, and J. Li, "A potential field based lateral planning method for autonomous vehicles," *SAE Int. J. Passeng. Cars - Electron. Electr. Syst.*, vol. 10, no. 1, pp. 24–34. Sept. 2016.